The Journal of Experimental Biology 202, 3523–3539 (1999)
Printed in Great Britain © The Company of Biologists Limited 1999
JEB2257

FUNCTIONAL MORPHOLOGY OF UNDULATORY PECTORAL FIN LOCOMOTION IN THE STINGRAY *TAENIURA LYMMA* (CHONDRICHTHYES: DASYATIDAE)

LISA J. ROSENBERGER[1,2,*] AND MARK W. WESTNEAT[2]

[1]*Department of Organismal Biology and Anatomy, University of Chicago, 1027 East 57th Street, Chicago, IL 60637, USA* and [2]*Department of Zoology, Field Museum of Natural History, Roosevelt Road at Lake Shore Drive, Chicago, IL 60605-2496, USA*

*Author for correspondence at address 2 (e-mail: ljrosenb@midway.uchicago.edu)

Accepted 21 September; published on WWW 29 November 1999

Summary

Rajiform locomotion is a unique swimming style found in the batoid fishes (skates and rays) in which thrust is generated by undulatory waves passing down the enlarged pectoral fins. We examined the kinematic patterns of fin motion and the motor patterns of pectoral fin muscles driving the locomotor system in the blue-spot stingray *Taeniura lymma*. Our goals in this study were to determine overall patterns of fin motion and motor control during undulatory locomotion, to discover how these patterns change with swimming velocity and to correlate muscle function with kinematics and pectoral morphology. Kinematic data were recorded from five individuals over a range of swimming speeds from 22 to 55 cm s^{-1} (0.9–3.0 *DL* s^{-1}, where *DL* is body disc length). Electromyographic (EMG) data were recorded from three individuals over a range of velocities (1.2–3.0 *DL* s^{-1}) at seven locations (four dorsal, three ventral) along the pectoral fin. As swimming velocity increases, fin-beat frequency, wavespeed and stride length increase, number of waves and reduced frequency decrease and fin amplitude remains constant. There is variability among individuals in frequency and amplitude at a given speed. An inverse relationship was found in which a high fin-beat frequency is associated with a low fin amplitude and a low fin-beat frequency is associated with a high fin amplitude. The motor pattern of undulatory locomotion is alternate firing activity in the dorsal and ventral muscles as the wave moves along the fin from anterior to posterior. Fin muscles are active along the entire length of the fin except at the lowest speeds. As swimming velocity and fin-beat frequency increase, the time of activation of posterior muscles becomes earlier relative to the onset of activity in the anterior dorsal muscles. The duration of muscle activity is longer in the ventral muscles than in the dorsal muscles, indicating that they play a central role in the power stroke of the fin-beat cycle. The anterior muscles (dorsal and ventral) are active for a relatively longer part of the stride cycle than the posterior muscles. Both the anterior position and the large duty factor of the anterior muscles reflect the role of these muscles in initial wave generation. Synchronous recordings of kinematic data with EMG data reveal that the anterior dorsal and middle ventral muscles do mostly positive work, whereas the dorsal and ventral posterior muscles do negative work at most swimming speeds.

Key words: kinematics, electromyography, swimming, muscle, biomechanics, rajiform locomotion, blue-spot stingray, *Taeniura lymma*.

Introduction

Research on the mechanics of aquatic locomotion in fishes has recently begun to focus on the fishes that use their pectoral fins for primary propulsion. Most of these studies have examined ray-finned fishes (Actinopterygii) of relatively recently derived groups such as labroids (Webb, 1973; Drucker and Jensen, 1996, 1997; Westneat, 1996; Walker and Westneat, 1997; Westneat and Walker, 1997), sunfishes (Centrarchidae, Gibb et al., 1994) and pufferfishes (Diodontidae, Arreola and Westneat, 1996; Tetraodontidae, Gordon et al., 1996). Little attention has been given to pectoral locomotion in the batoid fishes (electric rays, sawfishes, guitarfishes, skates and stingrays). Batoids exhibit two modes of pectoral swimming behavior: (1) undulatory locomotion, termed ‘rajiform’ (Breder, 1926), and (2) oscillatory locomotion, termed ‘mobuliform’ (Webb, 1994). Rajiform locomotion is performed by skates (Rajidae) and most stingrays (Dasyatidae) and involves undulatory waves that are propagated down the pectoral fins from anterior to posterior. Mobuliform locomotion occurs as the pectoral fins ‘flap’ up and down. The pelagic rays (eagle rays and manta rays) swim using this style. Although these modes are considered discrete categories (Breder, 1926; Lindsey, 1978; Webb, 1998), there is actually an undulation-to-oscillation continuum onto which different fishes fall, including many species of batoids. Some

rays, such as the dasyatids, are able to modify their locomotor style from undulation to oscillation in different locomotor situations. Beyond the identification of these broad categories, further research is necessary to understand the functional morphology of these locomotor styles.

The mechanisms of forward locomotion by fishes have been investigated through the use of models involving both steady-state and unsteady hydrodynamics. In the steady-state scheme, lift is created on both the up- and downstrokes by orienting the fin at an angle to the water (Blake, 1983a). Lift-based fins tend to be short-based and wing-like. Drag-based propulsion is created by performing a power stroke and a recovery stroke (Blake, 1983a) with fins that are broad-based and fan-like. These steady-state models do not provide complete descriptions of animal propulsion through fluids, however. Another way to model thrust propulsion by pectoral fins involves unsteady effects. The most common unsteady effect in fishes is an acceleration reaction, which resists both acceleration and deceleration of a body through a fluid. Thrust is generated when an added mass (the mass of the water flowing over the body) gives increased inertia to an accelerating body (Daniel, 1984). Batoids may use a combination of drag, lift and unsteady effects (acceleration reaction) to produce thrust during locomotion. In theory, drag-based locomotion is efficient at slow speeds, while lift-based locomotion is efficient at fast speeds (Vogel, 1994). Therefore, it is important to assess swimming over a range of biologically relevant speeds.

The biomechanics of batoid locomotion have been studied by several researchers (Marey, 1893; Magnan, 1930; Campbell, 1951; Klausewitz, 1964; Roberts, 1969; Daniel, 1988; Heine, 1992), who observed the general movement patterns of the pectoral fins of different species. Daniel (1988) used hydrodynamic theory to investigate how batoid pectoral fins operate. He examined undulatory locomotion in the skate *Raja eglanteria* using a combination of blade-element theory and unsteady airfoil theory. Daniel (1988) accounted for unsteady aspects of fluid motions as well as complex fin motions by combining these theories to investigate the energy requirements for flight with three-dimensional fins. He determined that skates primarily use unsteady effects during locomotion to produce thrust, and concluded that the shape of the pectoral fins, quantified by aspect ratio, minimizes the cost of transport. Daniel's (1988) work and the more qualitative studies cited above suggest a need for quantifying kinematic behavior over a range of swimming velocities to determine the way in which batoids increase their swimming speed.

Several studies have examined the relationship between locomotor kinematics and the muscle activity patterns responsible for locomotor movement. Together, these studies have provided insight into how muscles function to drive locomotor behavior, how the firing pattern changes with velocity and how muscles perform work during locomotion. Westneat and Walker (1997) examined pectoral fin electromyography in the bird wrasse *Gomphosus varius* and showed how fin motions during pectoral propulsion in these fishes are driven by the musculature of the pectoral fins. They found that the pectoral muscles did positive work at most speeds and a small amount of negative work at high speeds. Other studies have examined how muscles work in bending the body during axial undulation in fishes (Rome et al., 1993; Jayne and Lauder, 1995; Wardle et al., 1995) and found that the posterior muscles produce negative work. Studies of muscle function in bird (Dial et al., 1991; Tobalske, 1995) and insect (Mizisin and Josephson, 1987; Tu and Dickinson, 1994) flight revealed that these winged propulsors use negative work to control the wing movement. The undulatory pectoral fins of stingrays are designed very differently from teleost fins and other animal wings, providing an opportunity to investigate aquatic propulsion in an independently derived functional system.

The central goal of this study is to investigate the mechanics of undulatory locomotion in the stingray *Taeniura lymma* by applying the techniques of computer-aided video analysis and electromyography to reveal aspects of swimming kinematics and neuromuscular control. We ask the following questions. (1) What are the patterns of motion of the pectoral fins over a range of swimming speeds? (2) How do the motor patterns change with increasing swimming velocity? (3) How do the muscles function to produce specific swimming behaviors? Answers to these questions supply a foundation for comparative and evolutionary studies of aquatic locomotion in the diverse batoid fishes.

Materials and methods

Five blue-spot stingrays (*Taeniura lymma* Forsskål 1775) were used in this study, ranging in size (Table 1) from 15 to 18 cm disc length (*DL*, the length of the body disc from the tip of the snout to the base of the tail). Fishes were purchased from a Chicago fish wholesaler and maintained in aquaria at the Field Museum of Natural History, at a temperature of 22 °C. Rays were fed earthworms and commercial marine pellet food. They swam in a flow tank of 360 l and with working area dimensions of 30 cm×30 cm×120 cm for the kinematic and electromyographic experiments. Tank speeds ranged from 22 to 55 cm s^{-1}, equivalent to speeds of 0.9–3.0 *DL* s^{-1} for each individual. The speeds tested represent the low and high range of swimming velocity for this species. Typical swimming speeds in the aquaria and around coral reefs are between 1 and 2 *DL* s^{-1} (personal observation).

Table 1. *Morphometric data for* Taeniura lymma *individuals used in this study*

Individual	Disc length (cm)	Disc width (cm)	Circumferential length (cm)
T. lymma 1	16.3	14.3	24.0
T. lymma 2	15.8	13.7	22.4
T. lymma 3	14.9	14.0	22.5
T. lymma 4	17.9	15.6	24.6
T. lymma 5	17.1	15.4	24.3

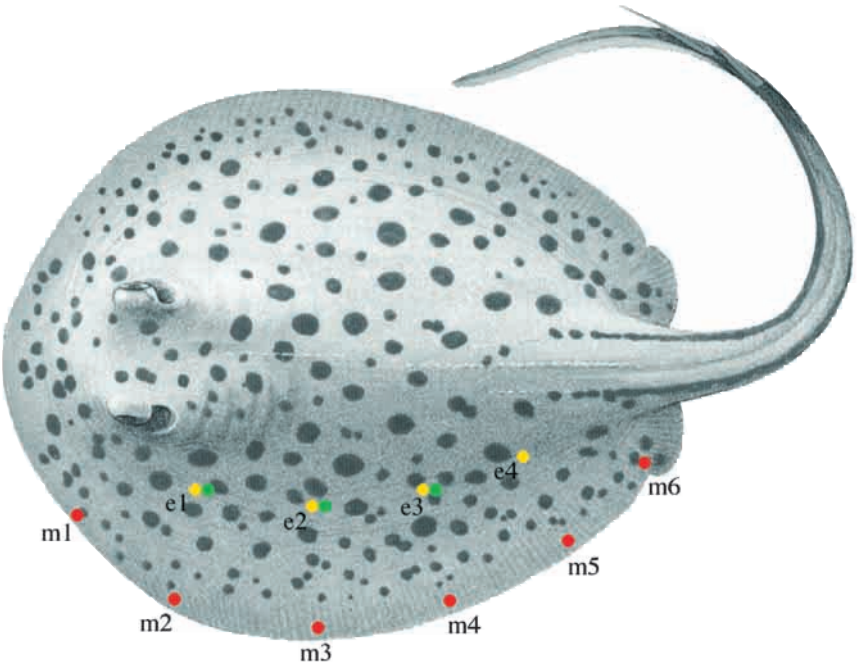

Fig. 1. Dorsal view of *Taeniura lymma* modified from Last and Stevens (1994). Aluminum clip markers were placed at six locations (m1–m6, in red) along the left pectoral fin for digitizing homologous points frame by frame. Electrodes were inserted into the muscles at seven positions, four dorsal (e1–e4, in yellow) and three ventral (e1–e3, in green). Dorsal and ventral muscle activity is distinguished in the text and graphs by referring to the dorsal muscle insertions as D1–D4 and the ventral muscle insertions as V1–V3. Anterior is to the left.

Morphology

Pectoral fin morphology was studied for the purpose of determining the appropriate positions for electrodes and aiding in the interpretation of EMG patterns for fin kinematics. We used gross dissection of the musculature to determine the structure of the different layers of muscle in the pectoral fins. Superficial dissection of dorsal and ventral surfaces as well as sectioning the fin provided details of muscle design. For a study of the skeleton, an X-ray of *Taeniura lymma* (AMNH 44076) was examined (courtesy of M. Carvalho). A specimen of *Potamotrygon motoro* (FMNH 94503) was cleared and stained using standard procedures of trypsin digestion and Alcian staining for cartilage (Dingerkus and Uhler, 1977).

Kinematics

Video recordings of rays swimming over a range of speeds in the flow tank allowed three-dimensional analysis of fin kinematics. A mirror positioned at 45° was placed inside the flow tank for observing dorsal and lateral views simultaneously. A Panasonic AG-450 S-VHS camera recorded images at a shutter speed of 1/1000 s and a frame rate of 60 images s^{-1}. Red aluminum clip markers were placed at six positions (m1–m6) along the left pectoral fin for digitizing homologous points frame by frame (Fig. 1). Fig. 2 shows images of *Taeniura lymma* swimming in the flow tank. A TelevEyes/Pro video scan converter with genlock superimposed video and computer images onto a Sony PVM-1340 monitor. Video recordings were played back for digitization with a Panasonic AG-1970 tape deck for five fin beats for each of five individuals at five swimming speeds, giving a total of 125 fin beats analyzed. Data were taken when the rays were swimming in the middle of the flow tank to minimize wall effects (Webb, 1993). A custom-designed digitizing program, developed by J. Walker, was used for recording 16 digitized points from both dorsal and lateral views, and for measuring the *x*, *y* and *z* coordinates of each point along the fin. Coordinate data were exported to Microsoft Excel 5.0 for calculation of the kinematic variables.

The following kinematic variables were calculated for each individual at all the recorded flow speeds: amplitude of fin waves, peak propulsive wavespeed, mean wavespeed over the entire fin, number of waves present along fin, fin-beat frequency, wavelength, phase velocity, stride length and reduced frequency. The amplitude of the waves was calculated as the average of the maximum upstroke and maximum downstroke distances in the dorsoventral direction for each of the marked points along the fin. The amplitude for each marker was standardized by disc width, corresponding to the width at each marker (e.g. marker 3 was standardized by width at the widest portion of the disc; see Fig. 1). Propulsive wavespeed (u) was determined as the distance that the wave traveled, in the middle one-third of the fin (between m2 and m4), divided by the time for it to move that distance. Mean wavespeed was computed as the distance the wave traveled (disc length) divided by the time for one complete wave to move down the fin. The number of waves present on the fin was calculated by dividing disc length by wavelength. Frequency (f) was computed as the number of fin-beat cycles per second. Wavelength was calculated as propulsive wavespeed divided by frequency. Phase velocity (U/u) determines the ratio of forward swimming speed (U) to propulsive wavespeed. Stride length (U/f) is the distance the fish traveled in one fin beat. Reduced frequency was determined using the equation (Vogel, 1994):

$$f_a = 2\pi nc/U,$$

where n is fin-beat frequency, c is the maximum chord of the

fin perpendicular to the central fin rays (in cm) and U is forward velocity (in cm s^{-1}).

Electromyography

Electromyographic (EMG) data were used to quantify muscle activity in swimming *Taeniura lymma*. EMG data were recorded from three individuals over a range of swimming speeds. Rays were anesthetized by putting 2 g of MS-222 in 1 l of water and incrementally adding the solution to a tank (with the ray inside) holding approximately 8 l of water until anesthesia was complete. Bipolar electrodes were constructed from 0.05 mm diameter, insulated, stainless-steel wire and threaded through a 25 gauge needle for implanting into the left pectoral fin of anesthetized rays. Electrode wires were run posteriorly to a suture at the base of the tail, where they were glued together to form a single cable. EMG data were measured at four locations (e1–e4) along the abductor (dorsal) muscle and at three locations (e1–e3) along the adductor (ventral) muscle (Fig. 1) in the superficial layers of the pectoral muscles (see below). To distinguish between dorsal and ventral muscles in the text and graphs, electrode positions in the dorsal muscles are referred to as D1, D2, D3 and D4, and those in the ventral muscles are referred to as V1, V2 and V3. Rays were allowed a minimum of 2 h to recover before the experiments began. EMG signals were amplified by a factor of 5000–10 000 by AM Systems (model 1700) amplifiers, filtered by a 100 Hz high-pass filter and recorded on a TEAC eight-channel DAT tape recorder. EMGs were digitized by an NB-MIO-16 analog-to-digital converter driven by LabVIEW virtual instrument software (National Instruments Corp., Austin, Texas, USA). Data were sampled at 5000 points s^{-1} $channel^{-1}$ and were analyzed using an eight-channel analysis algorithm custom-designed using LabView software (National Instruments).

Three complete fin beats were analyzed for each fish at five tank speeds, for a total of 45 fin beats analyzed. Thirty-three EMG variables, in five categories, were measured for each fin beat, including duration (ms) of muscle activity, onset time (ms) of other muscles relative to anterior dorsal muscle activity, mean signal amplitude (mV) of each burst of activity, rectified area of the EMG (in mV ms; calculated by multiplying the mean amplitude of the rectified spikes by the duration of the burst), onset times of dorsal muscles relative to minimum kinematic amplitudes and onset times of ventral muscles relative to maximum kinematic amplitudes. Duty factor of muscle activity (the percentage of the stride cycle that the muscle is active) and cycle onset of muscle activity (the percentage of the cycle time it takes for a muscle to fire in relation to the dorsal anterior fibers) were calculated from duration and relative onset data. Because of potential variation in electrode construction and insertion, comparisons of signal amplitudes or rectified areas among muscles should be interpreted with caution, although these variables were considered for overall patterns associated with swimming velocity.

Synchronized kinematics and EMG recordings

Video recordings were made simultaneously with EMG recordings to examine fin motions in lateral view for finding minimum and maximum amplitudes at three positions along the fin (anterior, m2; middle, m3; posterior, m4). Kinematic and EMG data were synchronized by using a 5 V square wave from a function generator pulsing at 8 Hz. This square wave was supplied to a channel on the EMG tape deck and to a flashing light-emitting diode on the video screen. The square wave was activated and a voice recording was entered on both video and EMG tape to distinguish swimming sequences of interest for easy synchronization. The square wave in the EMG recording and the flashing light in the video recording were matched to allow correlation of kinematics with motor patterns. This technique was used to determine relative EMG timing for kinematic events. Temporal error was minimized to within 8 ms (half a video interfield interval).

To correlate kinematic markers with electrode placement for determining relative timing, the anteroposterior position of

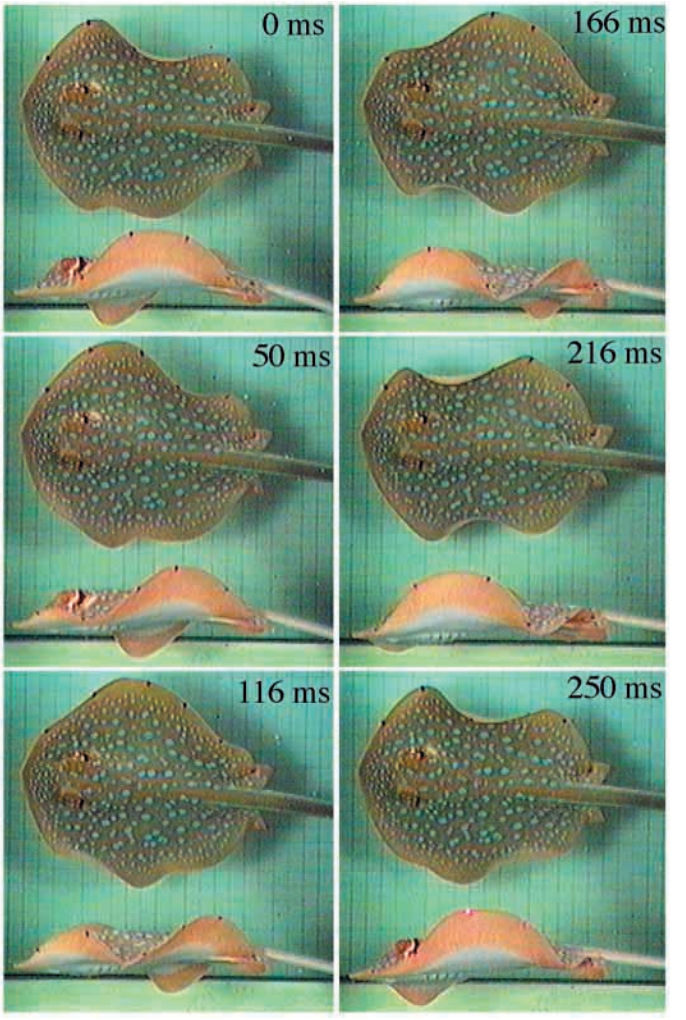

Fig. 2. Successive lateral and dorsal video images of *Taeniura lymma* swimming in a flow tank at approximately 2 *DL* s^{-1} (where *DL* is disc lengths). The dorsal view, at the top of each frame, is a reflected mirror view. *T. lymma* swims by propagating undulatory waves down the pectoral fins. Anterior is to the left.

each aluminum marker was found as a percentage of the length of the distal margin (circumferential length) of the pectoral fin (Fig. 1; Table 1) and the position of each electrode insertion point was found as a percentage of disc length (Fig. 1; Table 1). The wavespeed of fin motion and the speed of EMG signal propagation down the fin were constant at a given speed, allowing the onset of activity in the muscle directly controlling each fin marker to be calculated. Thus, the timing of activity in a particular muscle relative to its corresponding kinematic marker was determined. Data from three kinematic markers (m2, m3, m4) and six electrodes (D1, D2, D3, V1, V2, V3) were analyzed to determine when the dorsal muscles fired in relation to peak downstroke and when the ventral muscles fired in relation to peak upstroke.

Statistical analyses

We tested all kinematic and EMG variables for the strength of their relationship with swimming velocity by performing least-squares regressions of each variable on swimming speed. Least-squares regressions were used because swimming speed was a predictor of kinematic and EMG response variables. Individual variability in kinematics and EMG variables was considerable, so we tested the significance levels of individual variation using analysis of covariance (ANCOVA). In this model, the associations between kinematics and velocity and between EMG variables and velocity are compared among individuals to test for differences in slope and intercept. All analyses were performed using JMP 3.1 (SAS Institute). Once significance had been determined for all variables in each test, *P*-values were corrected using the sequential Bonferroni method (Rice, 1989) to negate inflated significance values due to multiple tests.

Results

Pectoral fin morphology

The pectoral girdle is unique in batoids, with the scapulacoracoid either fusing together dorsally by means of the suprascapula or articulating directly to the synarcual (fused vertebra) by means of a ball-and-socket joint (Compagno, 1973). In *Taeniura lymma* and *Potamotrygon motoro*, the fin radials are attached to the scapulacoracoid *via* three enlarged basal radials (Fig. 3A,B). These basal cartilages are the propterygium (expanded anteriorly), mesopterygium (small central element) and metapterygium (expanded posteriorly). All three basal radials support the enlarged pectoral fins and may or may not be segmented. The smaller fin radials extend out from the basal radials to the fin margin (aplesodic) in derived batoids and are segmented along their length. The radials are longest in the middle portion of the fin and become progressively shorter moving anteriorly and posteriorly.

Dissections of the pectoral fin musculature of *Taeniura lymma* reveal complex layers of muscle and connective tissue (Fig. 4). The dorsal (abductor) muscle used in elevating the fin (Fig. 4A) and the ventral (adductor) muscle used in depressing the fin are divided into superficial and deep layers (Fig. 4B),

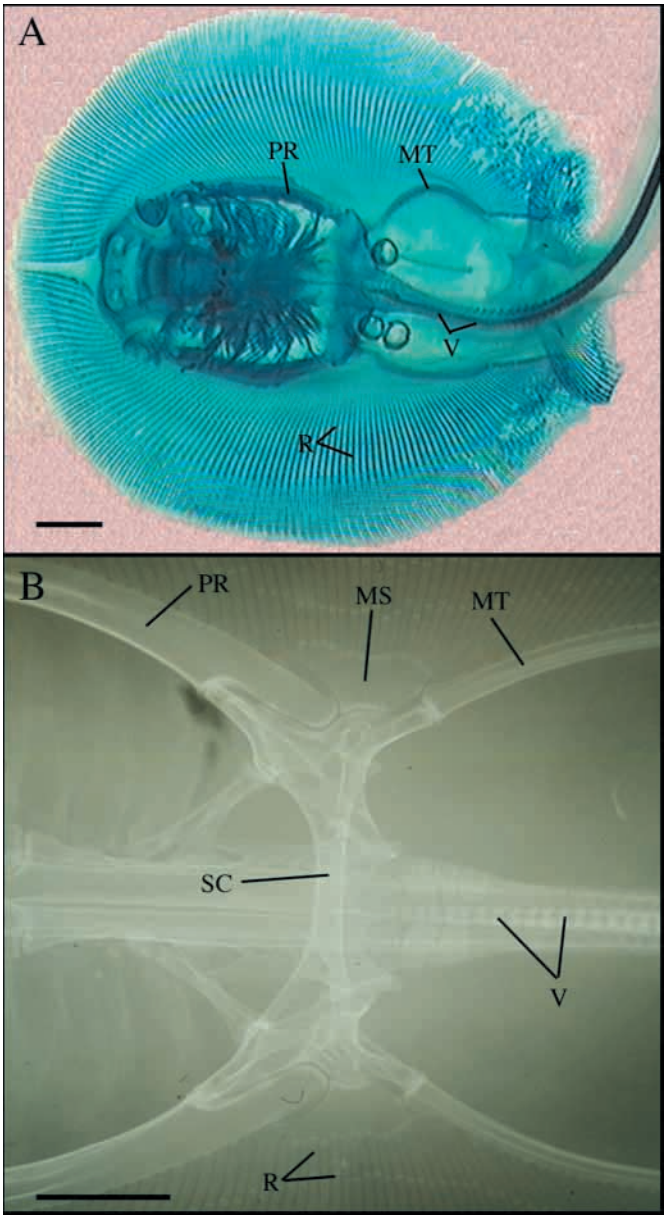

Fig. 3. (A) Dorsal view of a cleared and stained skeleton of *Potamotrygon motoro*, a species closely related to *Taeniura lymma*. Scale bar, 1 cm. (B) Radiograph of the pectoral girdle of *Taeniura lymma*. Scale bar, 0.5 cm. Anterior is to the left. MS, mesopterygium; MT, metapterygium; PR, propterygium; R, radials; SC, scapulocoracoid; V, vertebrae.

each surrounded by tendinous sheaths. Pectoral muscles originate on all three basal radials and run parallel to the fin radials. The muscles are thickest proximally and taper gradually to their insertion points. The superficial layers of muscle are greater in cross-sectional area proximal to the body than are the deep layers, and the ventral musculature is smaller in cross-sectional area than the dorsal musculature. The superficial muscles insert onto a tendinous sheath (surrounding the deep layers) at approximately half (ventrally) to three-fifths (dorsally) of the length to the fin margin, while the deep

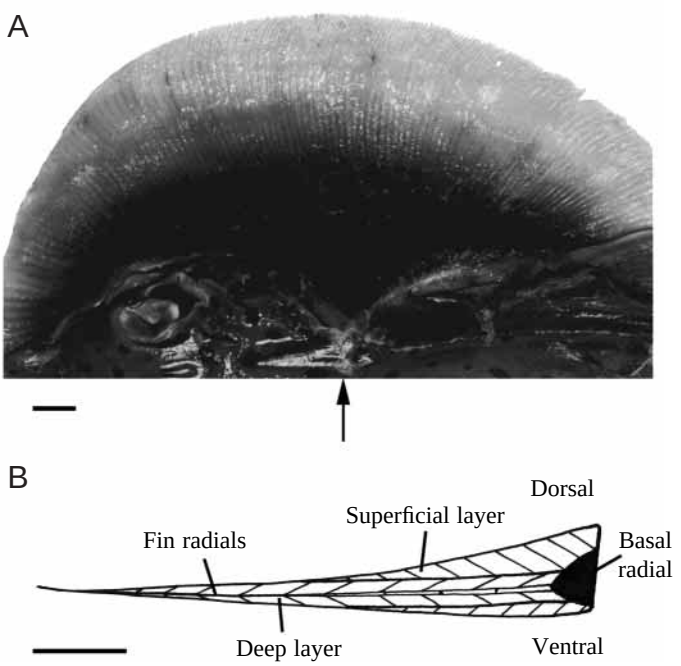

Fig. 4. (A) Dorsal view dissection of pectoral abductor muscles in *Taeniura lymma*. (B) Schematic drawing of a pectoral fin cross section (at arrow) showing superficial and deep muscles, fin radials and the basal radial. Scale bar, 1 cm.

muscles extend to the fin margin. The muscles of *T. lymma* are black in coloration to approximately half-way to the fin margin, where the superficial muscles end (Fig. 4A). This coloration has not been documented in any other stingray species. Lying proximally on top of the dorsal superficial muscle are thick bands of tendons that run along the anteroposterior axis of the pectoral fin.

Kinematics: trends with velocity

Taeniura lymma swims by passing waves along the pectoral fins from anterior to posterior (Fig. 2). Rays were able to maintain a steady position in the flow tank at all speeds. During steady forward swimming (no turning), both pectoral fins passed waves down the fins simultaneously. To increase swimming velocity, most individuals increased frequency and wavespeed, although there was high individual variability suggesting a trade-off between frequency and amplitude.

The five individuals shared general trends in kinematic variables, but variation between individuals was considerable (Tables 2, 3). As flow speed increased, frequency increased over the range 1.7–3.0 Hz (Fig. 5A; Table 2). Individual 2 showed the highest frequency at most speeds, while individual 1 showed the lowest frequency overall. Mid-disc fin wave amplitude (widest portion of fin, at marker m3), standardized by disc width, did not show a trend with velocity (Fig. 5B; Table 2), but did show individual variation (Table 3). The amplitude ranged from 0.14 to 0.28, with individual 1 having the highest amplitude and individuals 2 and 4 having the lowest amplitude. Amplitude along the fin increased from anterior (marker m1) to mid-disc (m3), where it reached its maximum value, then decreased slightly or remained constant from mid-disc to the posterior (m5) portion of the fin (Fig. 5C). Propulsive wavespeed increased steadily with increasing velocity with little individual variation (Fig. 6A; Tables 2, 3). Phase velocity increased with increasing speed, but remained below a value of 1, indicating that wavespeed was always faster than forward swimming speed (Fig. 6B; Table 2). Wavelength increased with velocity with no significant difference among individuals (Fig. 6C; Tables 2, 3). Stride length also increased similarly for all five individuals (Fig. 6D; Tables 2, 3), with little variation among them, suggesting that, although other kinematic variables were highly variable, individuals moved the same distance in a fin beat. The number of waves present along the fin was variable, but generally decreased as speed increased, ranging from 0.9 to 1.9 waves at any given time with a mean of 1.4 waves (Fig. 6E; Table 2). Reduced frequency decreased overall with increasing velocity

Table 2. *Statistical significance of least-squares regressions with* F*-ratios of kinematic data across all swimming speeds for* Taeniura lymma

Variable	Mean	S.D.	Range	Regression	r^2	*F* ratio
Frequency (Hz)	2.32	0.42	1.71–3.00	$y=0.53x+1.3$	0.57	29.2*
Amplitude[1] mid-disc	0.21	0.042	0.14–0.28	$y=0.021x+0.16$	0.10	2.75
Number of waves	1.36	0.23	0.87–1.93	$y=-0.24x+1.8$	0.39	14.05*
Propulsive wavespeed (cm s^{-1})	41.56	9.95	22.58–59.20	$y=15.5x+10.7$	0.88	156.3*
Mean wavespeed (cm s^{-1})	23.12	4.16	16.03–34.93	$y=5.88x+11.37$	0.73	58.4*
Wavelength (cm)	17.94	3.53	12.80–27.68	$y=2.83x+12.3$	0.23	6.69*
Phase velocity (*U*/*u*)	0.78	0.092	0.59–0.92	$y=0.086x+0.61$	0.32	10.21*
Stride length (cm)	79.31	33.72	28.24–144.00	$y=52.8x-26.2$	0.89	178.3*
Reduced frequency	6.90	1.52	4.54–10.81	$y=-1.99x+10.87$	0.62	36.3*

y is a measurement from the 'Variable' column and *x* is swimming speed.
*Significant ($P<0.05$), sequential Bonferroni-corrected.
[1]Amplitude = fin marker distance / disc width (% disc width).
U, swimming speed; *u*, propulsive wavespeed.

Table 3. F *ratios from analyses of covariance examining individual effects of kinematic variables*

Variable	Velocity	Individual	Velocity × individual
Frequency (Hz)	277.0*	4.61*	4.49*
Amplitude mid-disc (%)	9.31	6.42*	1.34
Number of waves	13.54*	0.31	0.53
Propulsive wavespeed (cm s^{-1})	276.0*	2.36	2.18
Mean wavespeed (cm s^{-1})	536.3*	4.04*	14.0*
Wavelength (cm)	10.45*	0.12	0.92
Phase velocity (*U*/*u*)	34.03*	3.49	3.46
Stride length (cm)	2159.0*	2.07	7.24*
Reduced frequency	292.1*	7.82*	3.84*

*Significant (P<0.05), sequential Bonferroni-corrected.
U, swimming velocity; *u*, propulsive wavespeed.

(Fig. 6F; Table 2), but remained above 4 at all speeds, indicating that unsteady effects are important.

Electromyography: motor patterns of rajiform locomotion

Electromyographic data revealed the basic motor pattern of rajiform locomotion in the blue-spot stingray to be alternate firing of the abductor (dorsal) and adductor (ventral) muscles as the wave propagates down the fin (Fig. 7). Both these muscles appeared to be equally active in fin deformation, and the muscles almost always fired in all parts of the fin from anterior to posterior. Occasionally, at low speeds, D2 and D4 muscle activity could not be detected, but activity was present at high speeds, indicating that the electrodes were functioning. Despite individual variability in EMG features, individuals shared general trends in motor patterns (Table 4), so data for the three individuals were combined for illustration.

The duration of muscle activity (Fig. 8A,B; Table 4) was fairly constant with increasing velocity in all positions. The anterior dorsal and ventral muscles (D1 and V1) fired for longer than the posterior muscles. The onset time of muscle activity (Fig. 8C,D; Table 4) relative to the anterior dorsal muscles (D1) revealed that the posterior muscles fired later in the stride cycle. All the muscles showed a decrease in relative onset (became earlier in timing) with increasing velocity. Duty factor (Fig. 9A,B; Table 4) increased with velocity in the anterior dorsal (D1, D2) and ventral muscles (V1) and the posterior ventral muscle (V3). The anterior muscles fired for proportionately longer in the ventral portion of the fin than in the dorsal portion. Cycle onset values (the onset time expressed as a fraction of stride duration) were greater than 1 at low speeds in the posterior muscles because the fin contains more than one wave along the fin. Cycle onset (Fig. 9C,D; Table 4) decreased with velocity in the mid-posterior dorsal muscles. The amplitude of muscle activity (Fig. 10A,B; Table 4) increased with speed in all muscles except the posterior dorsal and middle and posterior ventral muscles, for which amplitude which remained constant. The amplitudes were fairly low in voltage, ranging from 0.001 to 0.024 mV. The rectified area of muscle activity (Fig. 10C,D; Table 4) remained constant with

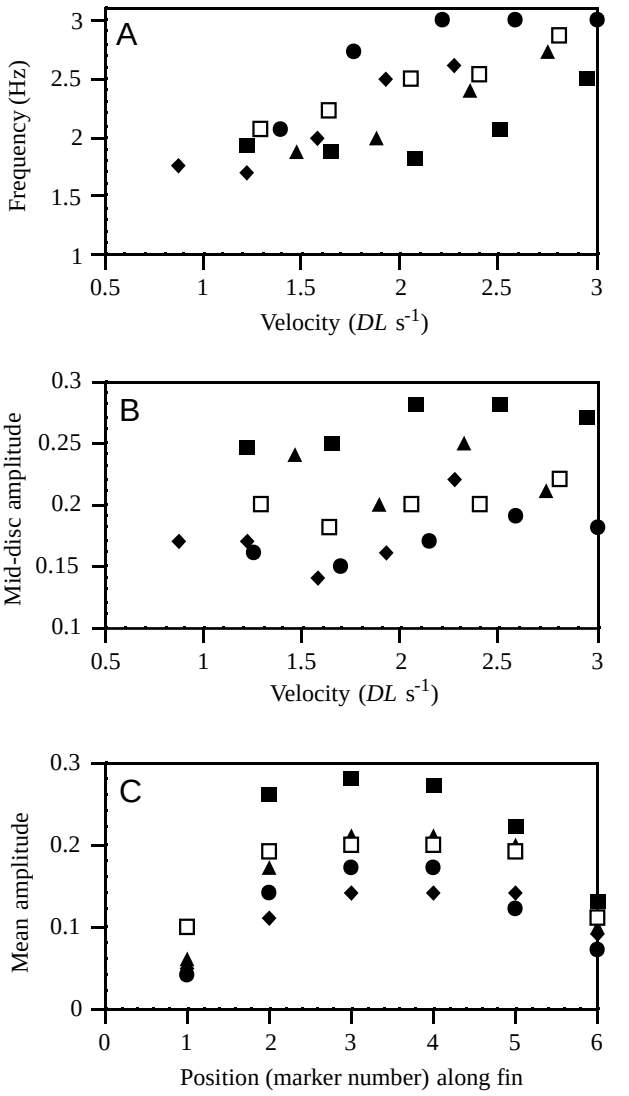

Fig. 5. Trends in (A) frequency and (B) mid-disc amplitude (at position m3), standardized by disc width, as swimming velocity increases. (C) Mean amplitude standardized by disc width (corresponding to marker position) at six positions along the pectoral fin. Numbers represent anterior to posterior positions, 1 being the most anterior, 6 being the most posterior. Symbols represent mean values for each individual, N=5 fin beats for each speed: ■, individual 1; ●, individual 2; ▲, individual 3; ◆, individual 4; □, individual 5.

increasing velocity in all but the mid-anterior dorsal muscle (D2).

Individual variation in muscle activity was high, as might be expected on the basis of kinematic variability (Table 5). The duration of activity in all ventral muscles and the posterior dorsal muscles (D4) was significantly different among individuals. The onset time of muscle activity was different for all muscles except D4. The area of muscle activity showed individual variation in the D4 and V2 muscles, and duty factor showed individual variability in the D4, V1 and V3 muscles. Amplitude was not significantly

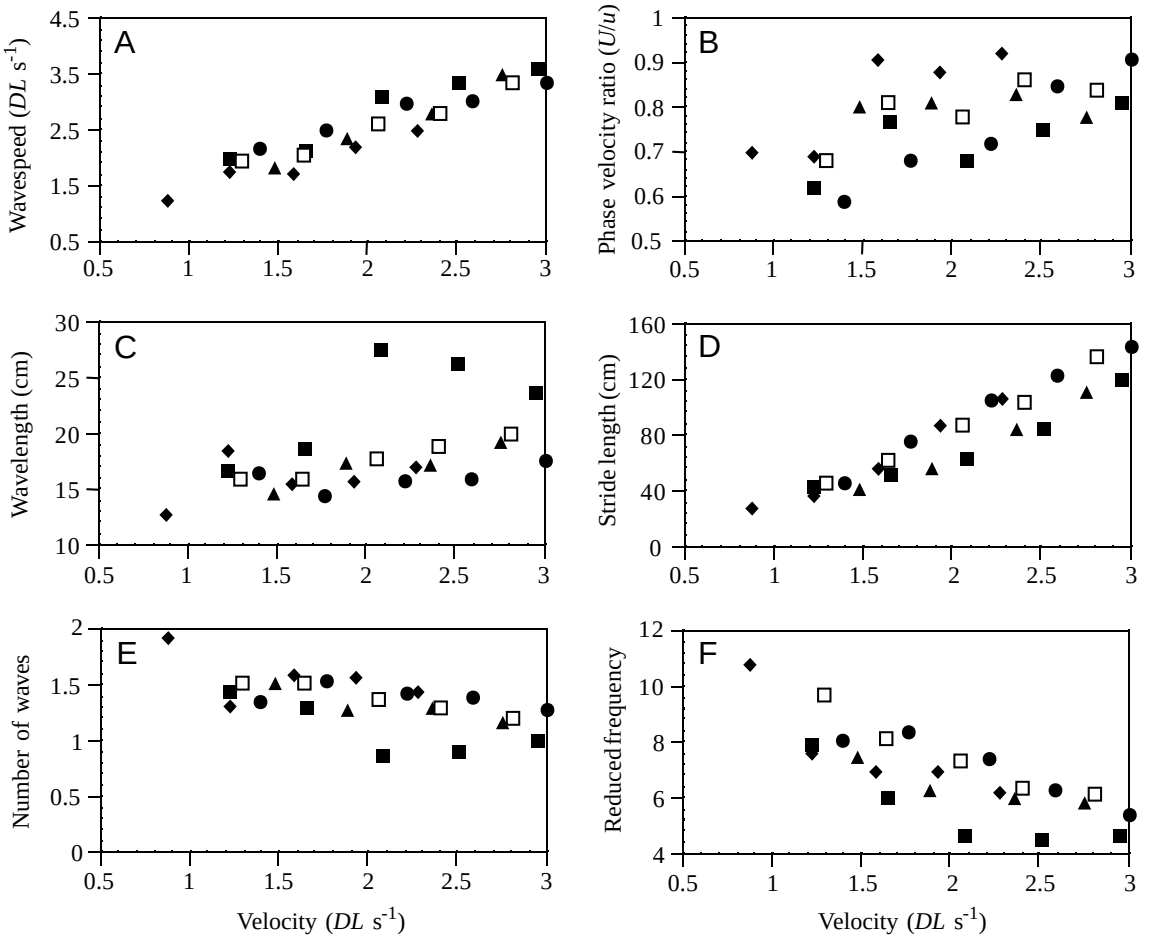

Fig. 6. Summary of kinematic data for *Taeniura lymma* as swimming velocity increases. (A) Propulsive wavespeed, standardized by disc length, increases with speed. (B) *U*/*u*, also known as the phase velocity ratio, generally increases with speed. Values below 1 indicate that the wavespeed is faster than the forward velocity. (C) Wavelength varies with velocity. (D) Stride length increases with velocity. (E) The number of waves along the fin decreases with speed. (F) Reduced frequency decreases with velocity and varies among individuals. Symbols represent means of each individual at each speed, *N*=5 fin beats for each speed: ■, individual 1; ●, individual 2; ▲, individual 3; ◆, individual 4; □, individual 5. *DL*, disc length; *U*, forward velocity; *u*, propulsive wavespeed.

different among individuals in any of the muscles tested (results not shown).

Synchronized kinematics and EMG

To understand how the muscles work to produce the kinematic behavior seen in the pectoral fins, the onset times of muscle activation relative to kinematic maxima and minima for the upstroke and downstroke were analyzed. We present the relative timing of excursions of three kinematic markers and EMG activity recorded by six electrodes (Fig. 11; Table 6). A detailed explanation is given below for a velocity of approximately $2\,DL\,s^{-1}$, followed by a discussion of trends with velocity.

As the anterior part of the fin (m2) reached its dorsal-most excursion (peak upstroke), the ventral muscle associated with the marker, V1, fired approximately 20 ms before the amplitude maximum (Fig. 11A). As the same part of the fin reached peak downstroke, the dorsal muscle (D1) fired 50 ms later (Fig. 11B). The middle portion of the fin (m3) reached peak upstroke approximately 20 ms before the ventral muscle (V2) fired (Fig. 11C) and reached its peak downstroke 5 ms after the dorsal muscle (D2) fired (Fig. 11D). In the posterior portion of the fin (m4), the ventral muscle (V3) fired 60 ms before peak upstroke (Fig. 11E) and the dorsal muscle (D3) fired 80 ms before peak downstroke (Fig. 11F).

All the muscle divisions, with the exception of the anterior dorsal muscle (D1), showed a speed-dependent trend of increasing the onset time in relation to their corresponding markers, although only the D3 and V3 onsets increased significantly. As the anterior position (m2) of the fin reached its peak upstroke, the onset of activity in the anterior ventral fiber (V1) increased from a negative value to a positive value (Fig. 11A). As m2 reached its peak downstroke, the onset of activity in D1 remained constant and positive at all velocities (Fig. 11B). The onset time of activity in the middle ventral muscle (V2) was mostly positive across velocity as the mid portion of the fin (m3) reached peak upstroke (Fig. 11C), while the onset of D2 (mid-anterior dorsal) changed from negative

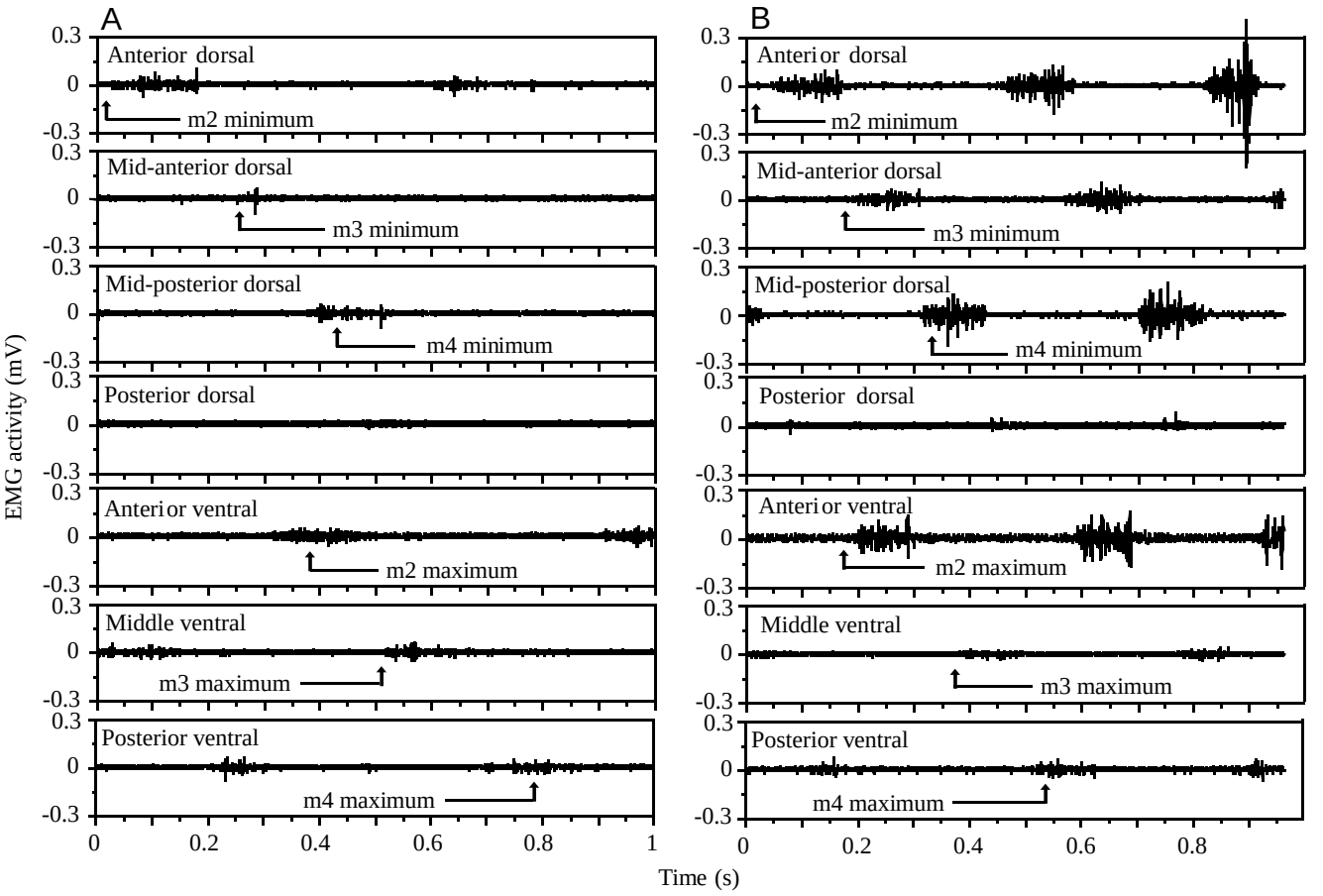

Fig. 7. Electromyographic (EMG) data illustrating the muscle activity for the pectoral fin undulation of *Taeniura lymma* at a low speed of 1.2 *DL* s^{-1} (A) and at a higher speed of 3.0 *DL* s^{-1} (B). The electrode recordings are taken from the following muscles: anterior dorsal (D1), mid-anterior dorsal (D2), mid-posterior dorsal (D3), posterior dorsal (D4), anterior ventral (V1), middle ventral (V2), posterior ventral (V3). The arrows below the EMG activity indicate the point during the fin-beat cycle at which the anterior, middle and posterior fin markers are at their maximum (peak upstroke) and minimum (peak downstroke) excursion. *DL*, disc length.

to positive as m3 reached its peak downstroke (Fig. 11D). Posteriorly (m4), as the fin reached both maximum (Fig. 11E) and minimum (Fig. 11F) amplitudes, the onset of activity in the V3 (posterior ventral) and D3 (mid-posterior dorsal) muscles remained negative as they increased in timing with velocity.

Discussion

This study presents the first integrated kinematic and electromyographic data set for locomotion of a batoid fish, the blue-spot stingray *Taeniura lymma*. We provide evidence for a trade-off between the use of frequency modulation and amplitude modulation to attain equivalent velocities. Correlation between kinematic and EMG patterns across swimming velocities reveals the mechanism by which rays modify their swimming behavior when increasing speed. We use the association between kinematic and EMG patterns, in combination with anatomical details of pectoral morphology, to propose a musculoskeletal mechanism of batoid undulatory locomotion. We conclude that a central role in the generation and propagation of undulatory waves on the pectoral fins is played by differential timing of contraction and differential work production by muscles along the anteroposterior axis of the body.

Kinematics: mechanisms of thrust by fin undulation

An aquatic animal moving through the water with an undulating body or fins can increase thrust and swimming speed by increasing undulatory frequency or by changing the wave characteristics of the undulation. Features of the undulatory wave that can be modulated are wave amplitude, wavelength and wavespeed. We found that, as velocity increased, *Taeniura lymma* increased its fin-beat frequency (Fig. 5A), propulsive wavespeed (Fig. 6A) and wavelength (Fig. 6C), but had a fairly constant fin amplitude (Fig. 5B). An increased frequency of the motion of a propulsor during an increase in velocity is a common feature of almost all swimming vertebrates, including sharks (Gray, 1968), eels (Gillis, 1998a), other fishes that use an undulating body or caudal fins (Videler, 1993; Wardle et al., 1995; Webb, 1988), fin-propelled fishes (Arreola and Westneat, 1996; Westneat,

1996), aquatic birds (Baudinette and Gill, 1985) and swimming mammals (Fish and Baudinette, 1999). The propulsive effect of increasing frequency and wavespeed is seen in the linear increase in stride length, which is the distance traveled during each undulatory cycle (Fig. 6D). Wavelength increased slightly with increasing swimming speed (Fig. 6C), resulting in fewer waves present along the fin.

Disc-width-specific amplitude did not correlate with swimming speed, suggesting that it is not as important as the other variables for increasing swimming velocities. Amplitude as a percentage of disc width increases along the fin from anterior to mid-disc, then remains constant before decreasing sharply at the posterior edge (Fig. 5C). One might predict that the amplitude would be greatest either anteriorly, as in triggerfishes (Wright, 1997), or posteriorly, as in the undulating bodies of eels (Gray, 1933; Gillis, 1998a). Instead, amplitude peaks in the central portion of the fin in a manner similar to the highly undulating fins of gymnotid fishes (Blake, 1983b). Blake (1983b) found that the amplitude increases from the anterior edge to a constant value that is maintained over

Table 4. *Statistical significance of least-squares regressions with* F *ratios of electromyographic data across all swimming speeds for* Taeniura lymma

Variable	Mean	S.D.	Range	Regression	r^2	*F* ratio
Duration D1 (ms)	124.6	25.2	80.6–193.4	$y=-9.43x+158$	0.14	6.45
Duration D2 (ms)	87.6	30.2	29.4–155.6	$y=0.42x+72$	0.02	1.15
Duration D3 (ms)	100.0	31.5	36.8–175.8	$y=-1.28x+145$	0.17	8.04
Duration D4 (ms)	82.1	44.2	14.6–179.6	$y=-0.98x+118$	0.04	2.29
Duration V1 (ms)	148.6	40.8	47.6–205.2	$y=0.28x+138$	0.01	0.30
Duration V2 (ms)	129.7	46.9	42.2–216.2	$y=-1.57x+186$	0.11	5.50
Duration V3 (ms)	104.1	45.2	22.0–208.6	$y=0.71x+79$	0.03	0.85
Onset of D2 relative to D1 (ms)	131.9	58.7	55.0– 293.0	$y=-3.65x+263$	0.46	28.1*
Onset of D3 relative to D1 (ms)	271.1	86.3	128.2–439.6	$y=-6.49x+500$	0.58	58.9*
Onset of D4 relative to D1 (ms)	332.0	93.7	172.2–527.4	$y=-6.73x+580$	0.46	31.9*
Onset of V1 relative to D1 (ms)	188.9	68.9	97.2–369.2	$y=-4.13x+335$	0.37	26.4*
Onset of V2 relative to D1 (ms)	342.4	99.2	197.8–562.6	$y=-7.14x+598$	0.51	41.7*
Onset of V3 relative to D1 (ms)	504.1	148.5	300.4–855.8	$y=-1.09x+889$	0.55	53.3*
Duty factor D1	0.29	0.06	0.17–0.46	$y=0.042x+0.20$	0.54	13.4*
Duty factor D2	0.21	0.08	0.05–0.45	$y=0.065x+0.08$	0.49	13.1*
Duty factor D3	0.23	0.06	0.10–0.40	$y=0.0095x+0.02$	0.05	1.0
Duty factor D4	0.19	0.10	0.03–0.35	$y=0.035x+0.13$	0.17	1.2
Duty factor V1	0.35	0.10	0.08–0.51	$y=0.11x+0.13$	0.85	25.8*
Duty factor V2	0.30	0.09	0.09–0.47	$y=0.036x+0.22$	0.30	1.7
Duty factor V3	0.25	0.12	0.04–0.48	$y=0.13x-0.02$	0.80	17.3*
Cycle onset of D2 relative to D1 (ms)	0.30	0.09	0.16–0.49	$y=-0.074x+0.45$	0.54	6.5
Cycle onset of D3 relative to D1 (ms)	0.61	0.12	0.39–0.85	$y=-0.12x+0.87$	0.60	7.6*
Cycle onset of D4 relative to D1 (ms)	0.77	0.14	0.53–1.12	$y=-0.051x+0.87$	0.21	1.
Cycle onset of V1 relative to D1 (ms)	0.43	0.09	0.23–0.62	$y=-0.27x+1.11$	0.50	2.1
Cycle onset of V2 relative to D1 (ms)	0.78	0.13	0.57–1.08	$y=-0.064x+0.91$	0.35	2.3
Cycle onset of V3 relative to D1 (ms)	1.13	0.18	0.83–1.61	$y=-0.27x+1.75$	0.75	6.3
Amplitude D1 (mV)	0.009	0.003	0.004–0.017	$y=0.00016x+0.004$	0.31	17.9*
Amplitude D2 (mV)	0.006	0.003	0.003–0.016	$y=0.00017x+0.003$	0.43	25.5*
Amplitude D3 (mV)	0.010	0.003	0.004–0.020	$y=0.00017x+0.004$	0.28	17.9*
Amplitude D4 (mV)	0.008	0.005	0.002–0.024	$y=0.00018x+0.001$	0.12	3.79
Amplitude V1 (mV)	0.011	0.004	0.003–0.023	$y=0.00023x+0.003$	0.30	19.7*
Amplitude V2 (mV)	0.006	0.003	0.001–0.014	$y=0.00008x+0.003$	0.07	2.77
Amplitude V3 (mV)	0.007	0.004	0.002–0.019	$y=0.00010x+0.003$	0.07	3.10
Area D1 (mV ms)	1.13	0.29	0.54–2.16	$y=0.011x+0.74$	0.15	8.09
Area D2 (mV ms)	0.57	0.40	0.18–2.46	$y=0.020x+0.15$	0.30	5.7*
Area D3 (mV ms)	0.93	0.37	0.37–1.96	$y=0.0049x+0.76$	0.02	1.13
Area D4 (mV ms)	0.70	0.59	0.13–2.35	$y=0.010x+0.34$	0.02	0.46
Area V1 (mV ms)	1.68	0.83	0.13–4.50	$y=0.033x+0.50$	0.17	9.45
Area V2 (mV ms)	0.78	0.60	0.10–2.66	$y=0.0028x+0.68$	0.002	0.06
Area V3 (mV ms)	0.74	0.49	0.11–2.44	$y=0.018x+0.104$	0.13	5.66

y is a measurement from the 'Variable' column and x is swimming speed.

*Significant ($P<0.05$), sequential Bonferroni-corrected.

D1, anterior dorsal; D2, mid-anterior dorsal; D3, mid-posterior dorsal; V1, anterior ventral; V2, middle ventral; V3, posterior ventral.

much of the fin length. As the wave reaches the posterior edge of the fin, the amplitude decreases. This decrease in amplitude posteriorly is believed to act as a reduction in cross-sectional depth, or narrow-necking, which minimizes the effects of recoil forces anteriorly (Blake, 1983b). *Taeniura lymma* fin morphology places this central portion of the fin as the lateral-

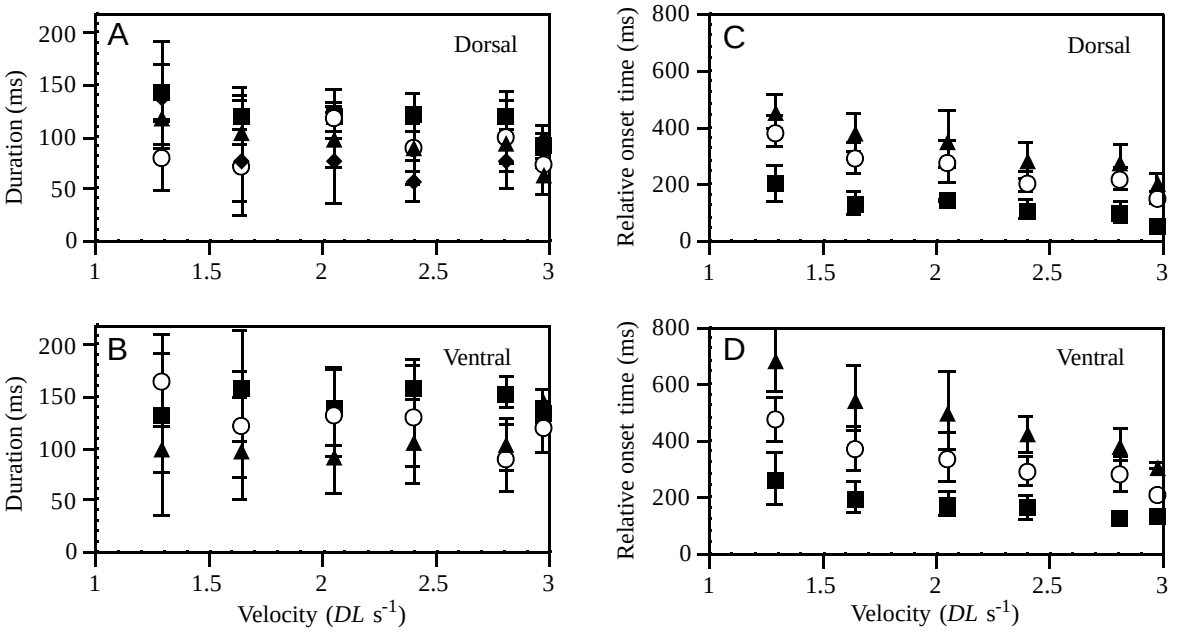

Fig. 8. (A,B) Trends in the duration of electromyographic (EMG) activity in the pectoral muscles of *Taeniura lymma* as a function of swimming velocity. The anterior muscle fibers are active for longer than all other muscle fibers, with the exception of the lowest velocity in the ventral muscle. (C,D) Trends in onset time of EMG activity relative to the anterior dorsal muscle fibers (D1), for all muscles except D1, as swimming velocity increases. The onset time of all muscle fibers decreases with increasing velocity. Values are means ± S.D. of each muscle fiber at each speed; *N*=3 fish at three fin beats per speed. Dorsal muscle fibers: ■, anterior (D1); ○, mid-anterior (D2); ▲, mid-posterior (D3); ◆, posterior (D4). Ventral muscle fibers: ■, anterior (V1); ○, middle (V2); ▲, posterior (V3). *DL*, disc length.

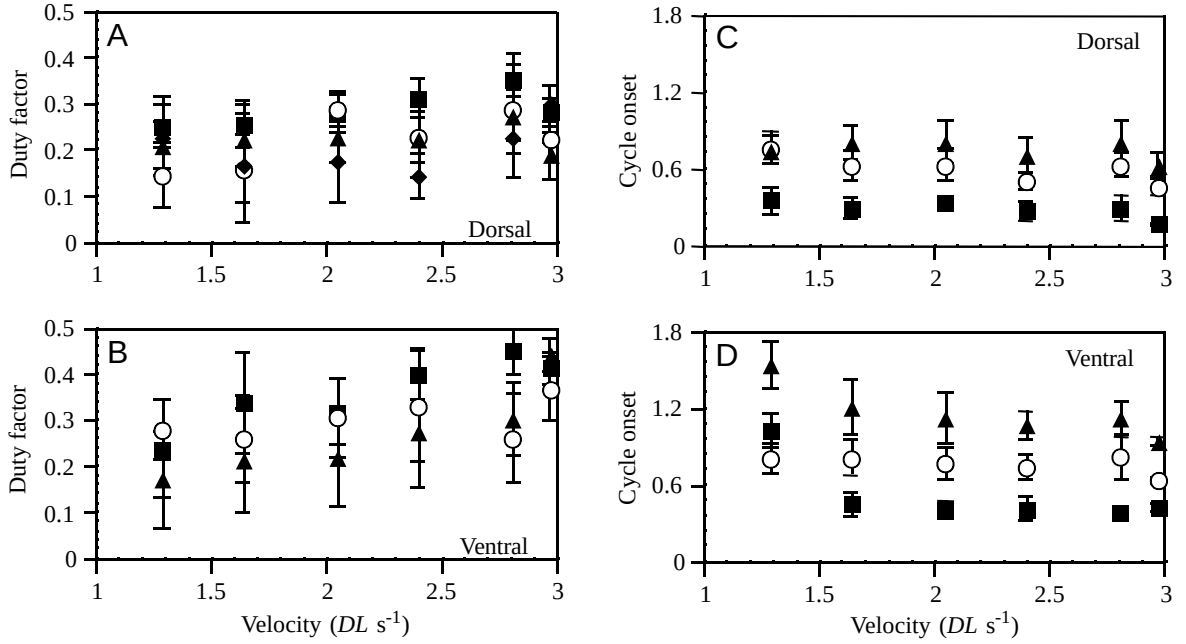

Fig. 9. (A,B) Duty factors of pectoral muscles, calculated as the muscle activity duration divided by total stride duration at each velocity. The ventral muscle fibers are active for a proportionately longer time than the dorsal fibers. (C,D) Onset times of pectoral muscle activity expressed as a fraction of the total stride duration at each velocity. Values are means ± S.D.; *N*=3 fish at three fin beats per speed. Symbols as in Fig. 8. *DL*, disc length.

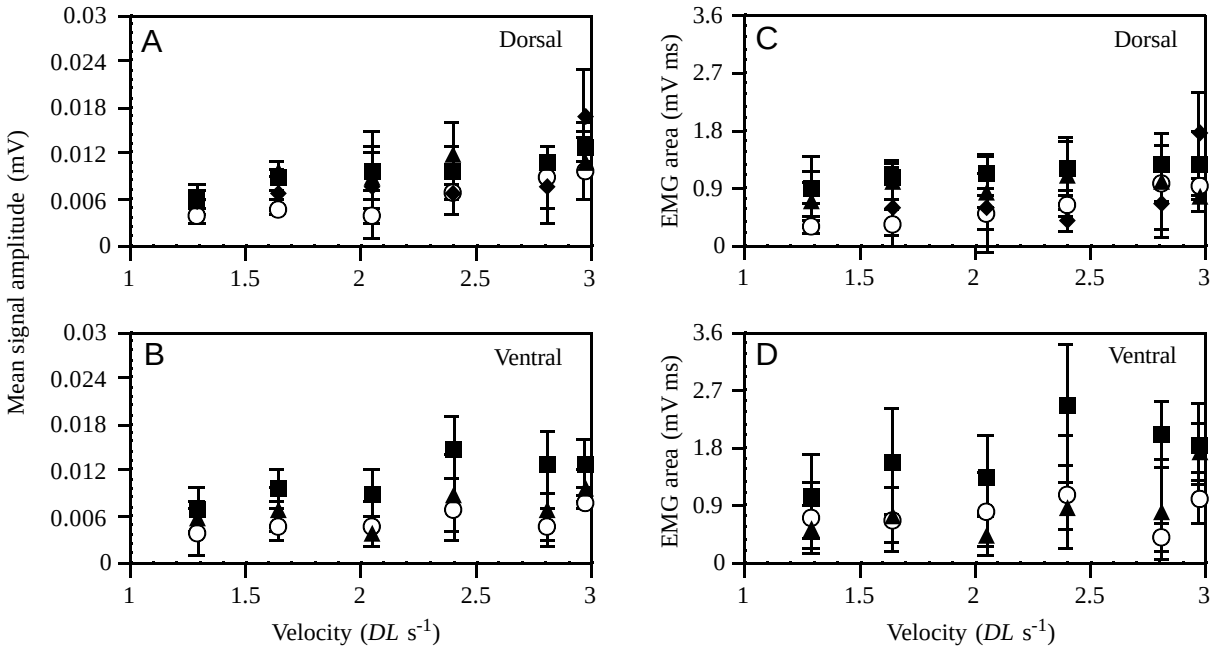

Fig. 10. (A,B) Trends in signal amplitude (mean voltage) of pectoral muscles as swimming velocity increases. Amplitudes increase with velocity in D1, D2, D3 and V1. (C,D) Trends in rectified, integrated area of electromyographic (EMG) activity in pectoral muscles of *Taeniura lymma* as swimming velocity increases. Area remains constant with increasing velocity, except for muscle D2. Values are means ± S.D.; *N*=3 fish at three fin beats per speed. Symbols same as in Fig. 8.

most propulsive element as well, so that maximal thrust is produced away from the center of mass on both sides. The generation of thrust away from the center of mass probably functions as a way of increasing turning moments for maneuverability.

Modulation of wavespeed is an important determinant of thrust in *Taeniura lymma*. We measured wavespeed in two ways (Table 2): an estimate along the central portion of the fin, where amplitude and thrust are maximal; and an estimate determined by the time required for a wave to travel the entire length of the fin. Wavespeed for the central fin ranged from 23 to 59 cm s^{-1}, whereas the overall mean wavespeed was much lower at 16–35 cm s^{-1}. We conclude that wavespeed is variable along the fin and that wavespeed is less than forward swimming velocity at the anterior and posterior edges. The ratio of swimming speed to wavespeed, termed phase velocity (Daniel, 1988) or 'slip', ranges from 0.6 to 0.9 in *T. lymma*, indicating that the speed of the wave rearward is always greater than the speed of the fish forward. This variable is the most likely determinant of increased stride length as velocity increases. Values of phase velocity are in the same range as those calculated for the skate *Raja eglanteria* (Daniel, 1988) and for eels (Gillis, 1996) and are based on propulsive wavespeed.

The reduced frequency parameter decreased with velocity, but remained above a value of 4 at all speeds (Fig. 6F). The reduced frequency parameter reveals the importance of acceleration reaction to thrust production. For many biological propulsors, values above 0.5 indicate that these unsteady effects are important during locomotion (Vogel, 1994). The high reduced frequencies at all speeds in the present study suggest that undulating pectoral fins primarily use an acceleration reaction, with some potential lift-based mechanisms, as they move through the water. Additional support for an acceleration reaction playing a key role in thrust production is the high ratio of fin flapping to forward velocity, assuming that the flow is attached to the fin chord. This corroborates Daniel's (1988) results from the skate *Raja eglanteria*, another undulating batoid. Daniel (1988) found that, to generate thrust with unsteady effects, there is a dependence on the number of propulsive waves and the reduced frequency parameter with an optimum for fin kinematics. He also determined that the aspect ratio of the fins is integral to the cost of transport, so that undulating fins have lower energy requirements as their aspect ratio decreases. Future studies using flow visualization will provide answers as to how the flow behaves with regard to the undulating pectoral fin and will extend our knowledge about the predominant generators of thrust in these fish.

A few kinematic variables revealed high variation among individuals, including frequency, amplitude and reduced frequency (Table 3). There appears to be a trade-off between fin-beat frequency and fin amplitude to produce identical swimming velocities. For instance, individual 1 had a relatively low fin-beat frequency and high fin amplitude, whereas individual 2 had a high fin-beat frequency and low fin amplitude (Fig. 5). Other individuals fell somewhere between these two extremes. This variation in kinematic behavior was qualitatively evident in the video recordings at all times. The behavioral differences described here are particular to the

Table 5. F *ratios from analyses of covariance examining individual effects of electromyographic variables*

Variable	Velocity	Individual	Velocity × individual
Duration D1 (ms)	1.88	0.43	1.10
Duration D2 (ms)	3.04	1.07	0.02
Duration D3 (ms)	2.85	0.26	0.12
Duration D4 (ms)	0.0004	12.04*	5.68*
Duration V1 (ms)	1.90	24.97*	11.65*
Duration V2 (ms)	0.89	5.55*	2.66
Duration V3 (ms)	0.01	39.03*	16.60*
Onset of D2 relative to D1 (ms)	52.68*	10.36*	5.27*
Onset of D3 relative to D1 (ms)	85.24*	9.33*	3.90*
Onset of D4 relative to D1 (ms)	41.48*	3.88	1.39
Onset of V1 relative to D1 (ms)	61.01*	21.34*	9.27*
Onset of V2 relative to D1 (ms)	64.79*	13.60*	8.09*
Onset of V3 relative to D1 (ms)	113.36*	17.17*	6.95*
Area D1 (mV ms)	3.45	0.27	0.46
Area D2 (mV ms)	12.01	0.62	1.26
Area D3 (mV ms)	0.12	0.86	1.40
Area D4 (mV ms)	2.08	12.01*	9.19*
Area V1 (mV ms)	10.16*	3.53	1.29
Area V2 (mV ms)	0.53	6.61*	2.20
Area V3 (mV ms)	5.04	0.77	0.63
Duty factor D1	17.58*	0.30	1.20
Duty factor D2	23.21*	0.47	0.30
Duty factor D3	5.04	0.23	0.45
Duty factor D4	5.74	8.76*	2.87
Duty factor V1	43.12*	14.45*	7.56*
Duty factor V2	11.87*	2.77	2.40
Duty factor V3	27.04*	20.15*	7.32*

*Significant ($P<0.05$), sequential Bonferroni-corrected.
Abbreviations for muscle positions are given in Table 4.

individual rays across all velocities. Low variation among individuals in stride length supports the idea that individuals can modify different kinematic variables, in this case frequency and amplitude, to move the same distance forward during a fin beat.

The high variability of frequency and amplitude seen among individuals could possibly be related to factors such as age, habitat or population differences. Unfortunately, the locality and age of the rays are unknown. Body size was not found to be a factor in the extreme variation between individuals 1 and 2 (Table 1), however, as both fit in the middle portion of the size range studied and they are very close to each other in disc size. Individuals 3 and 4 represent the small and large size extremes, respectively, and both show intermediate frequency and amplitude among the five individuals studied. Differences in behavior among individuals in the modulation of frequency and amplitude is also reflected in variation in motor patterns.

Motor patterns and muscle mechanics in batoid locomotion

EMG recordings (Fig. 7) showed that the dorsal and ventral muscles fired in an alternating sequential pattern as the wave moved down the fin from anterior to posterior. The muscles were active along the entire length of the fin except at the lowest speed, when the mid-anterior dorsal muscle (D2) and posterior dorsal muscle (D4) did not always fire during every fin beat. There are several ways in which muscles can modify their activity to alter kinematics and swimming velocity. These include changing the duration of muscle activity, the relative onset time of muscle activity and muscle amplitude. As swimming velocity increases, one might expect the duration of muscle activity to decrease with increasing frequency. In fact, the duration of muscle activity was fairly constant with increasing velocity (Fig. 8). Because frequency increases with speed (Fig. 5A), a constant duration results in a higher duty factor for the pectoral muscles (Fig. 9), which exhibit activity for a greater proportion of the stroke cycle at higher speeds. These results are different from those for fishes using undulatory bodies for propulsion. Jayne and Lauder (1995) showed that largemouth bass (*Micropterus salmoides*) decrease the absolute duration of lateral muscle activity, and that muscle duty factors decrease with increased speed. Undulating eels (Gillis, 1998b) decreased the duration of muscle activity, but duty factor was constant across swimming speeds. In *Taeniura lymma*, the increased duty factors of pectoral muscle probably contribute to increased transmission of force as a means of increasing wave speed.

The duration of muscle activity was variable at different positions along the body axis and was asymmetric dorsoventrally. *Taeniura lymma* also modulated the intensity of muscle contraction as frequency and swimming velocity increased. The anterior dorsal and ventral muscles fired for slightly longer (although not significantly so) than the posterior muscles (Fig. 8A,B). In *T. lymma*, this is due to the necessity for the anterior muscles to generate a relatively high-amplitude wave. In addition, the anterior muscles fired for longer in the ventral muscles than in the dorsal muscles, suggesting that the ventral muscles may generate greater force (Fig. 8A,B). Individual variation was found in the duration of activity in the ventral muscles, but not in the dorsal muscles (Table 5), suggesting that the duration of ventral muscle activity may be responsible for the individual differences seen in kinematic amplitude. These results are consistent with the qualitative observation that the downstroke may be used as a power stroke. Because the fish are slightly negatively buoyant, the greater power in the downstroke may generate lift to keep the body off the substratum.

Rather than changing the duration of muscle activity to increase swimming velocity, *Taeniura lymma* increases speed and fin-beat frequency by changing onset times in all the muscles along the fin, so that they fire closer together in time (Table 4). The rays also increase the intensity of the muscle activity amplitude in most of the muscles, although amplitude does not differ among individuals. The muscle onset times show the most variability among the three individuals of all the EMG parameters (Table 5), suggesting that this is important in influencing the variation seen in kinematic frequency.

Synchronizing kinematics with underlying motor patterns is critical to gaining a full understanding of the mechanisms

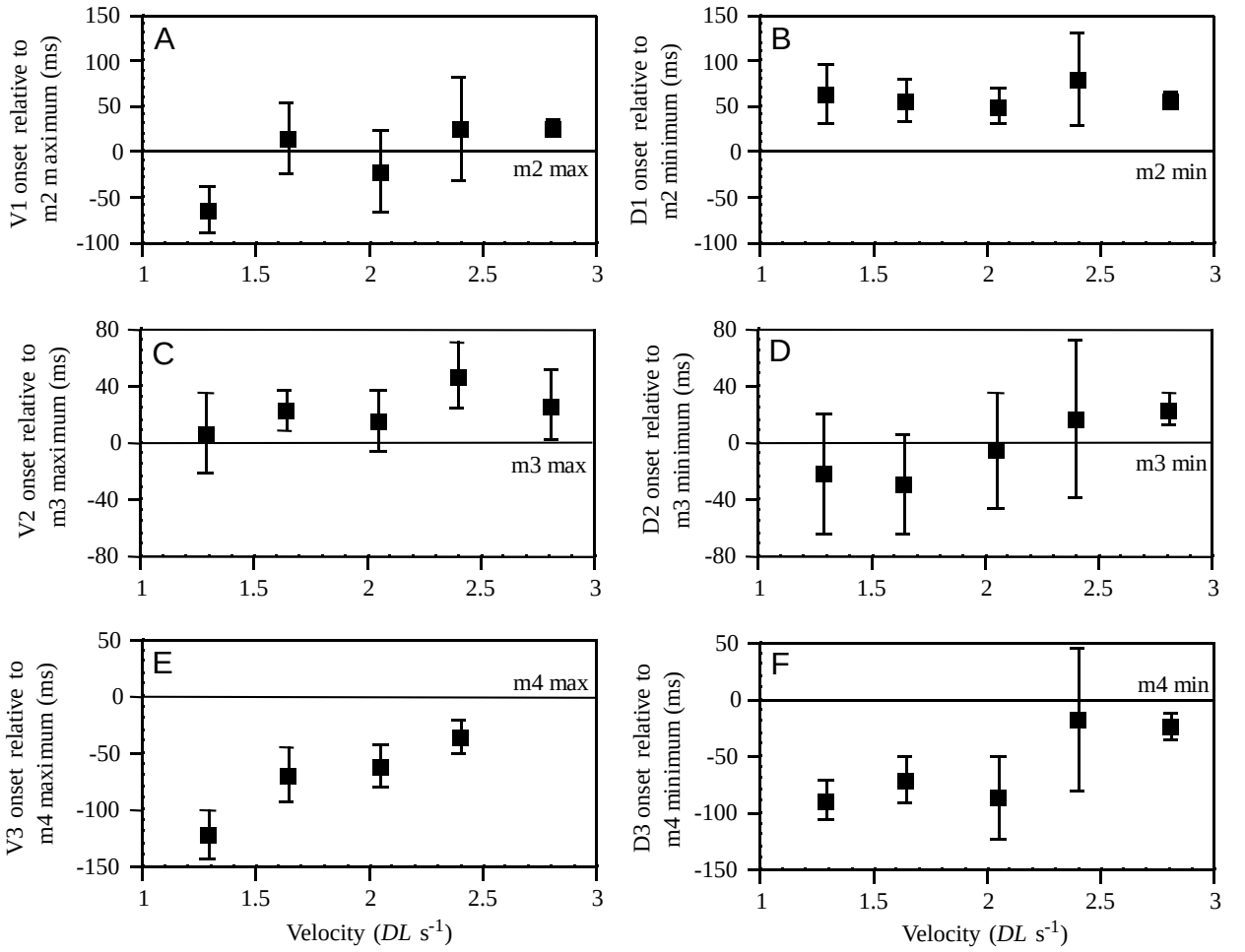

Fig. 11. Timing of electromyographic (EMG) variables relative to peak upstroke and downstroke at three positions (m2, m3 and m4) along the pectoral fins plotted against swimming velocity. *DL*, disc length. (A) Anterior ventral muscle, V1, onset time relative to m2 peak upstroke (m2 max); (B) anterior dorsal muscle, D1, onset time relative to m2 peak downstroke (m2 min); (C) middle ventral muscle, V2, onset time relative to m3 peak upstroke (m3 max); (D) mid-anterior dorsal muscle, D2, onset time relative to m3 peak downstroke (m3 min); (E) posterior ventral muscle, V3, onset time relative to m4 peak upstroke (m4 max); (F) mid-posterior dorsal muscle, D3, onset time relative to m4 peak downstroke (m4 min). Values less than zero indicate that negative work is being done; values greater than zero indicate positive work. Values are means ± S.D.; *N*=3.

driving a system such as the pectoral fins of *Taeniura lymma*. The timing of the onset of muscle activity relative to peak upstroke and downstroke reveals the degree to which muscles are active during the period of lengthening or shortening of the contraction cycle. We focused on the timing of muscle activity onsets relative to maximal fin excursions (peak upstroke and downstroke) to distinguish the type of work being performed by the muscles (Fig. 11). At low speeds, activity in the anterior ventral muscles began before peak upstroke, suggesting that negative work was performed for part of the upstroke, followed by positive work after the fin began the downstroke (Fig. 11A). In contrast, activity in the anterior dorsal muscles always began after peak downstroke, and only positive work was performed during the subsequent upstroke (Fig. 11B). Because there is no negative work being done anteriorly to slow the motion of the fin on the downstroke, fin deceleration could be caused by the viscosity of the water or the stiffness of the fin. Mechanical stiffness of the fin is a likely mechanism for fin reversal at peak downstroke when muscle activity has not yet been initiated. In the central part of the fin, where wavespeed was greatest, both dorsal and ventral muscles began firing close to the time of kinematic maxima (Fig. 11C,D). This indicates that almost all the work done by mid-body muscles was positive work during the shortening phase.

In stark contrast, posterior muscles on both the dorsal and ventral surfaces began activity 100 ms or more before peak upstroke and downstroke, respectively (Fig. 11E,F). The mean durations of activity in the posterior musculature were approximately 100 ms, indicating that a substantial portion of the force generation cycle occurs during muscle lengthening, with the production of net negative work. Muscle continues to produce force after EMG offset (Rome et al., 1993), allowing the possibility that some positive work is performed in this region, but most fish muscle shows peak force 30–50 ms after initial

Table 6. *Statistical significance of least-squares regressions with* F *ratios of muscle electromyographic onset timing relative to kinematic parameters across all swimming speeds for* Taeniura lymma

Variable	Mean	S.D.	Range	Regression	r^2	*F* ratio
V1 onset to m2 max (ms)	1.7	50.6	–93.6 to 107.6	$y=2.43x-84.4$	0.14	4.70
V2 onset to m3 max (ms)	26.4	24.4	–25.4 to 96.6	$y=1.08x-11.8$	0.12	3.86
V3 onset to m4 max (ms)	–69.2	36.9	–136.9 to –16.3	$y=4.07x-200$	0.71	26.7*
D1 onset to m2 min (ms)	62.0	32.8	–2.2 to 148.9	$y=0.26x+53$	0.004	0.15
D2 onset to m3 min (ms)	–5.1	44.4	–83.3 to 99.4	$y=2.15x-77.7$	0.17	6.69
D3 onset to m4 min (ms)	–58.2	48.1	–147.1 to 91.8	$y=2.97x-161$	0.26	10.8*

y is a measurement from the 'Variable' column and *x* is swimming speed.
*Significant ($P<0.05$), sequential Bonferroni-corrected.
D1, anterior dorsal; D2, mid-anterior dorsal; D3, mid-posterior dorsal; V1, anterior ventral; V2, middle ventral; V3, posterior ventral.
m2, m3, m4 max, peak upstroke; m2, m3, m4 min, peak downstroke.

muscle stimulation (Altringham et al., 1993). The posterior muscles did less negative work at higher speeds (Fig. 11E,F).

These results are in agreement with those from a broad range of studies on a diversity of undulating fishes (Gillis, 1998b; Jayne and Lauder, 1995; Wardle et al., 1995). Fishes with an undulating mode of locomotion are thought to use negative work in posterior myotomes to stiffen the body and to transmit forces posteriorly to the caudal fin (Long et al., 1994). Negative work regimes for locomotor muscle located posteriorly is thus a common feature for caudal fin mechanisms. Does the stingray *T. lymma* use a mechanism of increased stiffness posteriorly to increase propulsive thrust in the posterior region of the fin? This question is unresolved. Negative work for most caudal fin propulsors involves peak amplitude and wavespeed at the caudal fin, but *T. lymma* has peak amplitude and wavespeed in the central portion of the fin. Negative work is also associated with controlling the movement of a fin or wing, as in animals with an appendage used in a flapping motion (Tu and Dickinson, 1994). For example, if a wing is moving at a high frequency, negative work will decrease the velocity of the wing tip at maximal position (abduction or adduction) so that it can easily reverse direction. Negative work can also preload the muscles or tendons in order to increase stroke force in the direction that the muscles are firing (Westneat and Walker, 1997). Pectoral fin oscillation of the bird wrasse *Gomphosus varius* involves positive work at low speeds, but negative work at the highest velocities (Westneat and Walker, 1997). This is exactly the opposite of what is happening in the posterior region of the undulating stingray fin. Current studies of pectoral fin motion in a range of batoids with different aspect ratios and propulsive kinematics may resolve this issue.

Functional morphology of the batoid pectoral fin

Calvert (1983) presented the detailed morphology of the batoid pectoral fin and proposed the first biomechanical hypotheses for the function of this musculoskeletal system. She proposed a pinnate muscle model in which the superficial and deep muscles are bipinnately arranged with respect to a tendinous sheath between them. Because the superficial musculature is composed of red fibers, this part of the musculature was assumed to be responsible for slow steady swimming. To elevate or depress the fin, the superficial dorsal or ventral muscles contract, pulling on the dorsal tendon fascicle and tendinous sheath, which then pulls on the fin rays. The Calvert (1983) model predicts that the fin ray skeleton becomes a stiff, but bendable, sheet of cartilage because of the tendinous sheet covering the skeleton, so that once it is pulled by the tendons, the fin is bent upwards. The deep muscles are predicted to be pulled passively with the skeleton and play a role only in high-speed swimming or fast-starts from rest.

The placement of our EMG electrodes in the superficial muscles on both the dorsal and ventral surfaces (Fig. 4B) confirms the role of these superficial muscle layers in swimming at all measured swimming velocities. The relative role of the deep muscles remains unknown and should be tested by comparing EMG patterns in both the superficial and deep muscles in different swimming situations to determine when the superficial and deep muscles are active. Force transmission from muscle to the long rays of the fin support skeleton (Fig. 3) is an additional area for the development and testing of biomechanical models involving the contractile properties of muscle, the bending mechanics of calcified cartilage and the role of stiffness in the broad pectoral fins of batoid fishes.

In conclusion, our results on the kinematics and EMG activity of the pectoral fins in the blue-spot stingray *Taeniura lymma* allow us to interpret the mechanics of stingray pectoral fins during locomotion over a range of speeds. Swimming velocity is increased by increasing fin-beat frequency, wavespeed and duty factors for the pectoral muscles. Fin amplitude and muscle activity duration do not change with velocity. At the individual level, there is an apparent trade-off between frequency and amplitude to achieve a given swimming speed. Our data on the motor patterns of fin propulsion allow us to infer the role the muscles play in generating the movement required for undulatory fin propulsion. Future studies will examine other batoid species that exhibit pectoral undulation for comparison with *T. lymma*, as well as concentrating on species using oscillatory pectoral fin locomotion for understanding the diversity of locomotor mechanisms in batoid fishes.

We thank the Chicago Biomechanics Group, in particular M. Alfaro, R. Blob, J. Janovetz, M. LaBarbera, J. Walker and B. Wright, for their help on this project. Thanks to B. Wright for helpful discussion of the hydrodynamics of undulating fins. A. Summers, J. McEachran, B. Chernoff and the anonymous reviewers offered useful comments on this manuscript, and M. Carvalho provided us with the radiograph of the *Taeniura* pectoral girdle. This work was funded by a University of Chicago Hinds Fund grant to L.J.R., and Office of Naval Research grant N00014-99-0184 and National Science Foundation grants IBN-9407253 and DEB-9815614 to M.W.W.

References

Altringham, J. D., Wardle, C. S. and Smith, C. I. (1993). Myotomal muscle function at different points on the body of a swimming fish. *J. Exp. Biol.* **182**, 191–206.

Arreola, V. I. and Westneat, M. W. (1996). Mechanics of propulsion by multiple fins: kinematics of aquatic locomotion in the burrfish (*Chilomycterus schoepfi*). *Proc. R. Soc. Lond. B* **263**, 1689–1696.

Baudinette, R. V. and Gill, P. (1985). The energetics of flying and paddling in water: locomotion in penguins and ducks. *J. Comp. Physiol.* B **155**, 373–380.

Blake, R. W. (1983a). Median and paired fin propulsion. In *Fish Biomechanics* (ed. P. W. Webb and D. Weihs), pp. 214–247. New York: Praeger.

Blake, R. W. (1983b). Swimming in the electric eels and knifefishes. *Can. J. Zool*. **61**, 1432–1441.

Breder, C. M. (1926). The locomotion of fishes. *Zoologica* **50**, 159–297.

Calvert, R. A. (1983). Comparative anatomy and functional morphology of the pectoral fin of stingrays. Masters thesis, Duke University, Durham, NC, USA (139).

Campbell, B. (1951). The locomotor behavior of spinal elasmobranchs with an analysis of stinging in *Urobatis*. *Copeia* **1951**, 277–284.

Compagno, L. J. V. (1973). Interrelationships of living elasmobranchs. In *Interrelationships of Fishes* (ed. P. H. Greenwood, R. S. Miles and C. Patterson), pp. 15–61. New York: Academic Press.

Daniel, T. L. (1984). Unsteady aspects of aquatic locomotion. *Am. Zool*. **24**, 121–134.

Daniel, T. L. (1988). Forward flapping flight from flexible fins. *Can. J. Zool*. **66**, 630–638.

Dial, K. P., Goslow, G. E. and Jenkins, F. A., Jr, (1991). The functional anatomy of the shoulder of the European starling (*Sturnus vulgaris*). *J. Morph*. **207**, 327–344.

Dingerkus, G. and Uhler, L. D. (1977). Enzyme clearing of alcian blue stained whole vertebrates for demonstration of cartilage. *Stain Technol*. **52**, 229–232.

Drucker, E. G. and Jensen, J. S. (1996). Pectoral fin locomotion in the striped surfperch. I. Kinematic effects of swimming speed and body size. *J. Exp. Biol*. **199**, 2235–2242.

Drucker, E. G. and Jensen, J. S. (1997). Kinematic and electromyographic analysis of steady pectoral fin swimming in the surfperches. *J. Exp. Biol*. **200**, 1709–1723.

Fish, F. E. and Baudinette, R. V. (1999). Energetics of locomotion by the Australian water rat (*Hydromys chrysogaster*): a comparison of swimming and running in a semi-aquatic mammal. *J. Exp. Biol*. **202**, 353–363.

Gibb, A. C., Jayne, B. C. and Lauder, G. V. (1994). Kinematics of pectoral fin locomotion in the bluegill sunfish *Lepomis macrochirus*. *J. Exp. Biol*. **189**, 133–161.

Gillis, G. B. (1996). Undulatory locomotion in elongate aquatic vertebrates: anguilliform swimming since Sir James Gray. *Am. Zool*. **36**, 656–665.

Gillis, G. B. (1998a). Environmental effects on undulatory locomotion in the American eel *Anguilla rostrata*: kinematics in water and on land. *J. Exp. Biol*. **201**, 949–961.

Gillis, G. B. (1998b). Neuromuscular control of anguilliform locomotion: patterns of red and white muscle activity during swimming in the American eel *Anguilla rostrata*. *J. Exp. Biol*. **201**, 3245–3256.

Gordon, M. S., Plaut, I. and Kim, D. (1996). How puffers (Teleostei: Tetraodondtidae) swim. *J. Fish Biol*. **49**, 319–328.

Gray, J. (1933). Studies in animal locomotion. I. The movement of fish with special reference to the eel. *J. Exp. Biol*. **10**, 88–104.

Gray, J. (1968). *Animal Locomotion*. New York: W. W. Norton & Co. Inc.

Heine, C. (1992). Mechanics of flapping fin locomotion in the cownose ray, *Rhinoptera bonasus* (Elasmobranchii: Myliobatidae). PhD thesis, Duke University, Durham, NC, USA (289).

Jayne, B. C. and Lauder, G. V. (1995). Are muscle fibers within fish myotomes activated synchronously? Patterns of recruitment within deep myomeric musculature during swimming in largemouth bass. *J. Exp. Biol*. **198**, 805–815.

Klausewitz, W. (1964). Der lokomotionsmodus der Flugelrochen (Myliobatoidei). *Zool. Anz.* **173**, 110–120.

Last, P. R. and Stevens, J. D. (1994). *Sharks and Rays of Australia*. Australia: CSIRO.

Lindsey, C. C. (1978). Form, function and locomotory habits of fish. In *Fish Physiology*, vol. 7, *Locomotion* (ed. W. S. Hoar and D. J. Randall), pp. 1–100. New York: Academic Press.

Long, J. H., Jr, McHenry, M. J. and Boetticher, N. C. (1994). Undulatory swimming: how traveling waves are produced and modulated in sunfish (*Lepomis gibbosus*). *J. Exp. Biol*. **192**, 129–145.

Magnan, A. (1930). Les caracteristiques geometriques et physiques des poissons. Deuxieme partie. *Ann. Sci. Nat. Zool*. **13**, 134–269.

Marey, E. J. (1893). Des mouvements de natation de la raie. *C.R. Acad. Sci., Paris* **116**, 77–81.

Mizisin, A. P. and Josephson, R. K. (1987). Mechanical power output of locust flight muscle. *J. Comp. Physiol*. A **160**, 413–419.

Rice, W. R. (1989). Analyzing tables of statistical tests. *Evolution* **43**, 223–225.

Roberts, B. L. (1969). The buoyancy and locomotory movements of electric rays. *J. Mar. Biol. Ass. U.K.* **49**, 621–640.

Rome, L. C., Swank, D. and Corda, D. (1993). How fish power swimming. *Science* **261**, 340–343.

Tobalske, B. W. (1995). Neuromuscular control and kinematics of intermittent flight in the European starling (*Sturnus vulgaris*). *J. Exp. Biol*. **198**, 1259–1273.

Tu, M. S. and Dickinson, M. H. (1994). Modulation of negative work output from a steering muscle of the flowfly *Calliphora vicina*. *J. Exp. Biol*. **192**, 207–224.

Videler, J. J. (1993). *Fish Swimming*. London: Chapman & Hall.

Vogel, S. (1994). *Life in Moving Fluids*. Princeton: Princeton University Press.

Walker, J. A. and Westneat, M. W. (1997). Labriform propulsion in fishes: kinematics of flapping aquatic flight in the bird wrasse *Gomphosus varius* (Labridae). *J. Exp. Biol*. **200**, 1549–1569.

Wardle, C. S., Videler, J. J. and Altringham, J. D. (1995). Tuning in to fish swimming: body form, swimming mode and muscle function. *J. Exp. Biol*. **198**, 1629–1636.

Webb, P. W. (1973). Kinematics of pectoral fin propulsion in *Cymatogaster aggregata*. *J. Exp. Biol*. **59**, 697–710.

Webb, P. W. (1988). Simple physical principles and vertebrate aquatic locomotion. *Am. Zool*. **28**, 709–725.

Webb, P. W. (1993). The effect of solid and porous channel walls on steady swimming of steelhead trout *Oncorhynchus mykiss*. *J. Exp. Biol*. **178**, 97–108.

Webb, P. W. (1994). The biology of fish swimming. In *Mechanics and Physiology of Animal Swimming* (ed. L. Maddock, Q. Bone and J. M. V. Rayner), pp. 45–62. Cambridge: Cambridge University Press.

Webb, P. W. (1998). Swimming. In *The Physiology of Fishes*, 2nd edition (ed. D. H. Evans), pp. 3–24. New York: CRC Press.

Westneat, M. W. (1996). Functional morphology of aquatic flight in fishes: Mechanical modeling, kinematics and electromyography of labriform locomotion. *Am. Zool*. **36**, 582–598.

Westneat, M. W. and Walker, J. A. (1997). Motor patterns of labriform locomotion: kinematic and electromyographic analysis of pectoral fin swimming in the labrid fish *Gomphosus varius*. *J. Exp. Biol*. **200**, 1881–1893.

Wright, B. (1997). Oscillation *versus* undulation in balistiform locomotion. *Am. Zool*. **37**, 26A.